Aqueous extracts of *Sanghuangporus vaninii* induce S-phase arrest and apoptosis in human melanoma A375 cells

TAIHEN YU[1], SHI ZHONG[2], YUQING SUN[2], HAIYAN SUN[3], WEIGUO CHEN[3],
YOUGUI LI[2], JIANXUN ZHU[2], LONGXI LU[4] and JINXI HUO[2]

[1]Department of Radiology, Zhejiang Provincial People's Hospital, Affiliated People's Hospital of Hangzhou Medical College,
Hangzhou, Zhejiang 310014; [2]Institute of Sericultural and Tea, Zhejiang Academy of Agricultural Sciences, Hangzhou,
Zhejiang 310021; [3]Haining Economic Crop Technical Service Station, Haining Agricultural and Rural Bureau, Haining,
Zhejiang 314400; [4]Department of Environment & Health, Zhejiang Provincial Center for Disease Control and Prevention,
Hangzhou, Zhejiang 310051, P.R. China

Abstract. *Sanghuangporus vaninii*, also called 'Sanghuang' mushroom in Chinese, has various medicinal uses, but its effects on human melanoma cells have not been reported. The present study investigated the inhibitory ability and potential anticancer mechanism of the aqueous extracts of *S. vanini* (SH). The results revealed that SH inhibited the proliferation of A375 human melanoma cells in a dose-dependent manner, and flow cytometry analysis suggested that SH induced A375 cell cycle arrest at S phase and apoptosis. Reverse transcription-quantitative PCR, western blotting and immunofluorescence analyses indicated that SH induced S-phase arrest by upregulating p21 expression, and p21 inhibited the expression of cyclin-cyclin-dependent kinases complexes at both the RNA and protein levels. In addition, SH induced apoptosis of A375 cells by inhibiting the expression levels of the anti-apoptosis gene *Bcl-2*. Therefore, the results suggested that SH may be a potential candidate for the treatment of human melanoma, thus providing new ideas for developing drugs that target melanoma.

Introduction

Melanoma is one of the most aggressive types of cancer with an unpredictable course of disease. It accounts for 4% of all skin cancer cases but is responsible for 75% of deaths caused by these malignancies (1). Surgical removal is the best treatment for localised melanoma. For patients with metastatic disease, surgical treatment alone will not be curative, and chemotherapy and targeted therapy are necessary (2). However, the prognosis for patients treated by chemotherapy is unsatisfactory, and the side effects are serious, and the targeted therapy is limited to specific genotype patients (2). Therefore, effective drugs should be developed for the treatment of melanoma.

Sanghuangporus spp., also called 'Sanghuang' in China, are a well-known medicinal mushroom (3). Sanghuang have been used in Chinese traditional medicine for >2,000 years for the treatment of various diseases such as haemorrhage, haemostasis and diseases related to female menstruation (4). In recent years, modern pharmacological researches have revealed that *Sanghuangporus* spp. have multiple functions, such as anti-carcinogenesis, anti-inflammatory, anti-oxidative, anti-fungal and immunomodulatory activities (5,6). The extracts of *S. rimosus* have antiproliferative and apoptotic activities on human colorectal carcinoma HCT116 cells (7). The total ethanol extracts of *S. igniarius* have antitumor activities against gastric cancer SGC-7901 cells through a mitochondria-dependent pathway (8). Im *et al* (9) found that the extracts of *S. vaninii* are cytotoxic to murine melanoma B16-F10 cells at 25-750 mg/ml. Bae *et al* (10,11) demonstrated that polysaccharides from *S. gilvus* can inhibit forestomach carcinogenesis in mice and the proliferation of murine melanoma cells. Protocatechualdehyde induces S-phase arrest and apoptosis by stimulating the p27^{KIP1}-CyclinA/D1-cyclin-dependent kinase 2 (CDK2) and mitochondrial apoptotic pathways in HT-29 cells (12). 3,4-Dihydroxybenzalactone isolated from *S. linteus* suppresses human non-small cell lung carcinoma migration and invasiveness via the ROS-mediated PI3K/AKT/MAPK/MMP and NFκB signalling pathways (13). 3,4-Dihydroxybenzalacetone isolated from *S. obliguus* promotes anti-melanogenesis by downregulating melanosome maturation and transportation in murine melanoma B16F10 cells and human epidermal melanocytes (14). The extracts of *S. baumii* exert antitumour effects on human melanoma A375 cells *in vitro* and *in vivo* (15). *S. gilvus*-derived

Correspondence to: Dr Longxi Lu, Department of Environment & Health, Zhejiang Provincial Center for Disease Control and Prevention, 3399 Binsheng Road, Hangzhou, Zhejiang 310051, P.R. China
E-mail: lxilu@cdc.zj.cn

Dr Jinxi Huo, Institute of Sericultural and Tea, Zhejiang Academy of Agricultural Sciences, 298 Desheng Road, Hangzhou, Zhejiang 310021, P.R. China
E-mail: huojx@zaas.ac.cn

protocatechualdehyde induces G_0/G_1-phase arrest and apoptosis in murine B16-F10 cells (16). Therefore, Sanghuang has important inhibitory effects on melanoma. However, the effect of *S. vaninii* on human melanoma has not been reported. The present study revealed that aqueous extracts of *S. vaninii* fruiting body (referred as SH) acted as potential inhibitors of melanoma by inhibiting the proliferation of A375 cells and inducing cell cycle arrest and apoptosis.

Materials and methods

Cells and kits. The human melanoma A375 cell line was obtained from the Institute of Biochemistry and Cell Biology of the Chinese Academy of Sciences. The cells were cultured in RPMI-1640 medium (Thermo Fisher Scientific, Inc.) at 37˚C with 5% CO_2. The medium was supplemented with 10% FBS (Thermo Fisher Scientific, Inc.), penicillin (100 μg/ml) and streptomycin (100 μg/ml). MTT was obtained from Sigma-Aldrich (Merck KGaA). The Dead Cell Apoptosis kit with FITC Annexin V and PI was obtained from Thermo Fisher Scientific, Inc.

Preparation of aqueous extracts of S. vaninii fruiting body. The fruiting body of *S. vaninii* was cultivated at the Sericultural Research Institute of Zhejiang Academy of Agricultural Sciences (Hangzhou, China). The dried fruiting body powder was extracted with boiling water for 2 h. The supernatant was collected after centrifugation at 8,000 x g at room temperature for 10 min. The supernatant was lyophilised to obtain extract powders. The content of total polysaccharides and polyphenols was 5.51 and 23.00%, respectively. The major polyphenols were 3,4-dihydroxybenzalacetone, phellibaumin D and interfungin B (17).

Cell proliferation assay. Cell proliferation was determined by trypan blue staining and the inhibitory ratio was measured by MTT-based colorimetric assay as described by Zhong *et al* (16). Briefly, cells at the exponential growth phase were dispensed into a 96-well microplate at 100 μl/well. After 24 h, 100 μl of different concentrations of SH were added to prepare final concentrations of 50, 100, 200 and 400 μg/ml. Sterile water (0.1% DMSO) was used as control. The cells were cultured at 37˚C for 24, 36 and 48 h for cell counting. The supernatants of each well were obtained, and 50 μl of 0.25% trypsin was added into each well. After incubation at 37˚C for 5 min, the supernatants were re-added to the corresponding well to stop cell digestion. Cell suspensions (~20 μl) were transferred into a new 1.5 ml centrifuge tube with 20 μl of 0.4% trypan blue solution. After mixing, 20 μl cell suspension was added to a cell counting plate for counting with an automatic cell counter (IC1000; Countstar; ALIT Life Science Co., Ltd.). Cells cultured for 48 h were used for the MTT assay. The cells were incubated at 37˚C with 50 μl of MTT solution (1 mg/ml) for 2 h, and the resulting crystals were dissolved in DMSO. The absorbance at 570 nm was recorded to assess the formation of formazan. Inhibitory ratio (%) = [1-absorbance (test)/absorbance (control)] x 100%, where the test and control correspond to treated and untreated cells, respectively.

Cell cycle and apoptosis analysis. The cell cycle phase was measured by assessing the DNA content via flow cytometry as previously described by Zhong *et al* (16). Briefly, A375 cells (1x10^5 cells/well) were incubated at 37˚C with SH at final concentrations of 0 (control), 200 and 400 μg/ml for 48 h. The proportion of cells at different phases was determined using a flow cytometer (Cytomics FC 500 MCL; Beckman Coulter, Inc.). MultiCycle AV software (CXP V2.3 WIN7, C30309; Phoenix Flow Systems, Inc.) was used for analysis. Apoptosis rate was measured by staining with Annexin V-FITC (5 μl) and PI (5 μl) at 4˚C for 15 min. Annexin V$^-$/PI$^-$ (lower left quadrant) cells were alive cells, Annexin V$^+$/PI$^-$ (lower right quadrant) cells were early apoptotic cells, Annexin V$^+$/PI$^+$ (upper right quadrant) cells were late apoptotic cells and Annexin V$^-$/PI$^+$ (upper left quadrant) cells were necrotic cells. The proportion of cells was determined using a flow cytometer (Cytomics FC 500 MCL; Beckman Coulter, Inc.) with MultiCycle AV software (CXP V2.3 WIN7, C30309; Phoenix Flow Systems, Inc.). All experiments were performed in three biological duplicates.

Reverse transcription-quantitative (RT-q)PCR analysis. Total RNA was isolated from A375 cells treated with or without SH (400 μg/ml) for 6 and 48 h using the Takara MiniBEST universal RNA extraction kit (Takara Bio, Inc.). PrimeScript RT reagent kit with gDNA Eraser (Takara Bio, Inc.) and SYBR® Fast qPCR Mix (Takara Bio, Inc.) were used for the CFX96 real-time PCR system (Bio-Rad Laboratories, Inc.). All operations were performed in accordance with the manufacturer's instructions. The thermocycling conditions consisted of initial denaturation at 95˚C for 30 sec, followed by 40 cycles at 95˚C for 5 sec and 60˚C for 30 sec. GAPDH was used as an internal reference gene, and gene expression was quantified using the comparative $2^{-\Delta\Delta Cq}$ method (18). PCR primer sequences are summarised in Table I.

Western blot analysis. A375 cells treated with or without SH (400 μg/ml) for 48 h were collected for western blot analysis as previously described (12). Briefly, the total proteins were extracted using the SD-001 buffer (Invent Biotechnologies, Inc.) and supplemented with protein phosphatase inhibitor (Beijing Solarbio Science & Technology Co., Ltd.), and the protein concentrations were determined using a BCA protein assay kit. A total of 40 μg protein/lane was separated via 4-12% SDS-PAGE and then transferred to a polyvinylidene difluoride membrane. After blocking with 5% BSA (Merck KGaA) for 1 h at room temperature, membranes were incubated with the corresponding primary antibodies at 4˚C overnight. Subsequently, membranes were washed with PBS three times and incubated with the corresponding secondary antibodies at room temperature for 1 h. Primary antibodies (1:1,000) against p21 (cat. no. ab188224), CyclinD (cat. no. ab28283), CDK2 (cat. no. ab32147), CDK4 (cat. no. ab131469), CDK6 (cat. no. ab131469), Bcl-2 (cat. no. ab32124) and β-actin (cat. no. ab8226) were obtained from Abcam. The secondary antibody was Alexa Fluor 790-conjugated goat anti-rabbit IgG H&L (1:10,000; cat. no. ab175781; Abcam). The membranes were washed with PBS three times at room temperature, and the protein signals were visualised using the ChemiDoc touch imaging system (Bio-Rad Laboratories, Inc.) with Image Lab touch software (version 1.2; Chameleon Power).

Immunofluorescence analysis. A375 cells on a slide were fixed in 4% paraformaldehyde in PBS for 20 min at room

Table I. Primers used for reverse transcription-quantitative PCR.

Gene	Forward primer (5'-3')	Reverse primers (5'-3')
TGFB	GGACCAGTGGGGAACACTAC	AGAGTCCCTGCATCTCAGAGT
Smad2	CCATACCAAGGTCTCTTGATGGT	ACTGTGAAGATCAGGCCAGC
Smad4	GCAGTCCTACTTCCAGTCCAG	CCCATCTGAGTCTAATGCTACC
p21	AGCGACCTTCCTCATCCACC	AAGACAACTACTCCCAGCCCCATA
p53	AGCTTTGAGGTGCGTGTTTGTG	TCTCCATCCAGTGGTTTCTTCTTTG
p27	AAAAGCAACAGAAACCTATCCTCAC	ATTCAAAACTCCCAAGCACCTC
Cyclin A	TGGAAAGCAAACAGTAAACAGCC	GGGCATCTTCACGCTCTATTT
Cyclin B	GCAGCACCTGGCTAAGAATGT	GCCTTGGCTAAATCTTGAACT
Cyclin C	GCAGGACATGGGCCAAGAAGA	TATCCACAGAAAGCTCAGCAAACCA
Cyclin D	CCCTCGGTGTCCTACTTCAAATGT	GGAAGCGGTCCAGGTAGTTCAT
Cyclin E	GCCAGCCTTGGGACAATAATG	CTTGCACGTTGAGTTTGGGT
CDK1	GGATGTGCTTATGCAGGATTCC	CATGTACTGACCAGGAGGGATAG
CDK2	CCAGGAGTTACTTCTATGCCTGA	TTCATCCAGGGGAGGTACAAC
CDK3	CCAGCTCTTTCGTATCTTTCGT	TTCCTGGTCCACTTAGGGAAG
CDK4	ATGGCTACCTCTCGATATGAGC	CATTGGGGACTCTCACACTCT
CDK5	GGAAGGCACCTACGGAACTG	GGCACACCCTCATCATCGT
CDK6	TCTTCATTCACACCGAGTAGTGC	TGAGGTTAGAGCCATCTGGAAA
CDK7	ATGGCTCTGGACGTGAAGTCT	GCGACAATTTGGTTGGTGTTC
Rb	TTGTAACGGGAGTCGGGAGA	CAGCGAGCTGTGGAGGAG
E2F1	CACTTTCGGCCCTTTTGCTC	GTGCTCTCACCGTCCTACAC
DP1	ATGGCTCAGGGAACTGTTGG	GGTCACTGGCAGAGAACCTT
Bad	TTGGGGTGAGACCTGTGCG	CTCAGTCTCCCCTCAGAACCC
Bik	CATTCCAAAGAATCGAAGTCC	AATGTCTGAAGTAAGACCCCTCT
Bax	CCCGAGAGGTCTTTTTCCGAG	CCAGCCCATGATGGTTCTGAT
Bid	AGGAAGCCAAACACCAGTAGG	TGTGAACCAGGAGTGAGTCGG
Bim	TTTCTTGCGTTTCTCAGTCCG	CGCCACTACCACCACTTGATT
Bcl-xs	TCCCCATGGCAGCAGTAAAG	TCCACAAAAGTATCCTGTTCAAAGC
Bak	GCAGGCTGATCCCGTCC	CTGCGGAAAACCTCCTCTGT
Bcl-2	GGTGGGGTCATGTGTGTGG	CGGTTCAGGTACTCAGTCATCC
Bcl-xl	GCTGGGACACTTTTGTGGAT	GAGCCCAGCAGAACTACACC
Bcl-w	CTTTGTCTTTGGGGCTGCAC	CCATCCACTCCTGCACTTGT
Ras	AAGTGTGTGCTCTCCTGACG	CACAAGGGAGGCTGCTGAC
Raf	CAACTGATTGCACTGACTGCC	CCTGGAATTGCTCTGGGGTT
MEK1	CTTCGCAGAGCGGCTAGG	CAGCCCGGGATTCCCTTC
ERK1	GAGATGGATGTGGGTTCCAGTC	TTCTCATCGTAGCCACTCACC
GAPDH	GGACCTGACCTGCCGTCTAG	GTAGCCCAGGATGCCCTTGA

CDK, cyclin-dependent kinase; E2F1, transcription factor E2F1; DP1, transcription factor DP-1.

temperature, and then washed with PBS for 3 times. Cells were blocked with 3% BSA (Merck KGaA) for 30 min at room temperature, and then primary antibodies against CyclinD (cat. no. ab28283) and Bcl-2 (cat. no. ab32124) (both 1:200; Abcam) were added at 4˚C overnight. Subsequently, the slides were washed with PBS and incubated with DyLight 488-conjugated goat anti-rabbit IgG (1:200; cat. no. BA1127; Wuhan Boster Biological Technology, Ltd.) for 1 h at room temperature. The slides were mounted with DAPI-containing medium (C1002; Beyotime Institute of Biotechnology) for counterstaining of nuclei and then observed under a fluorescence microscope (Nikon Eclipse 80i; Nikon Corporation) at x100 magnification.

Statistical analysis. Data were expressed as the mean ± SD. Statistical analysis was performed using SPSS 16.0 software (SPSS, Inc.). One-way ANOVA was used to analyse statistical differences between groups under different conditions, followed by Tukey's post-hoc test. $P < 0.05$ was considered to indicate a statistically significant difference.

Results

SH inhibits proliferation of A375 melanoma cells. To examine the effects of SH on melanoma cells, A375 cells were treated with different concentrations of SH (0, 50, 100, 200 and 400 µg/ml) for 24, 36 and 48 h (Fig. 1). As shown in Fig. 1A
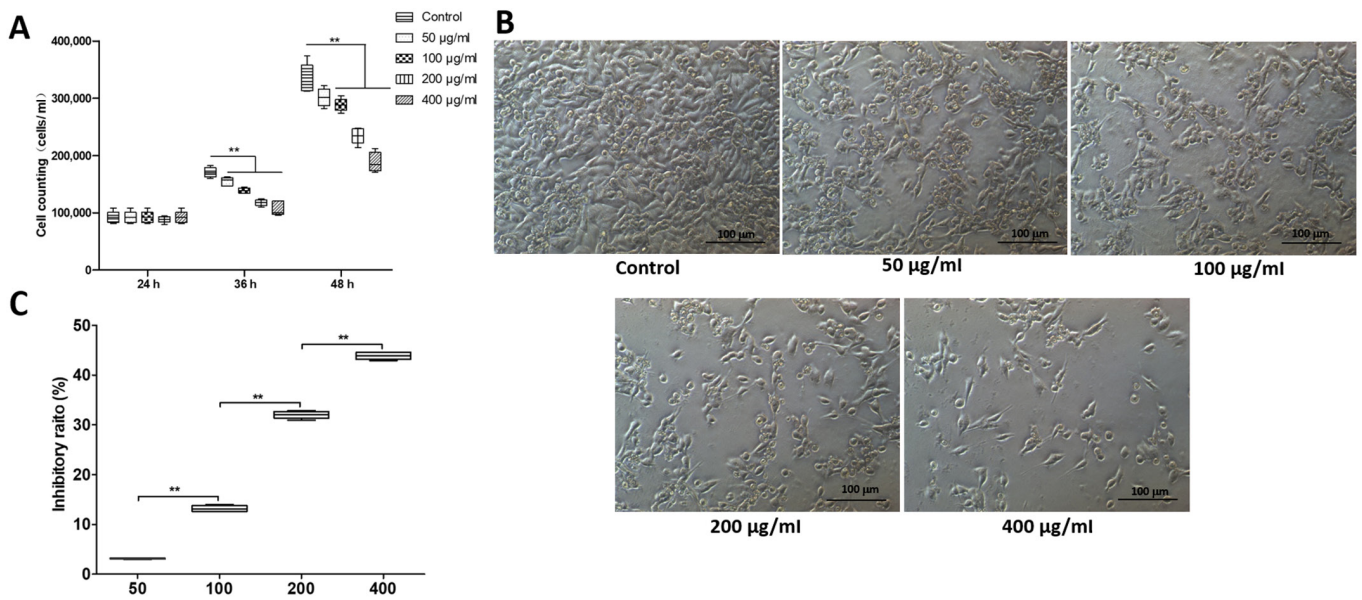
Figure 1. Inhibitory effect of SH on A375 cells *in vitro*. (A) Cell counting of A375 cells under treatment with various concentrations of SH (0-400 µg/ml) at 24, 36 and 48 h. (B) Morphological observation of A375 cells under treatment with various concentrations of SH (0-400 µg/ml) at 48 h. Scale bar, 100 µm. (C) MTT colorimetric analysis of A375 cells under treatment with various concentrations of SH (0-400 µg/ml) at 48 h. Values are presented as the mean ± SD (n=5 each group). **P<0.01. SH, *Sanghuangporus vaninii* extract.

and B, treatment of A375 cells with SH for 36 and 48 h significantly decreased cell viability compared with the control group in a dose-dependent manner. Particularly, 400 µg/ml SH effectively inhibited proliferation of A375 cells, along with a significant inhibitory ratio of >43% (Fig. 1B and C). Hence, SH suppressed the proliferation of A375 cells *in vitro*, suggesting that SH may be used as a cell proliferation inhibitor for the treatment of melanoma.

SH induces cell cycle arrest at the S phase and apoptosis. For further investigations on the inhibitory mechanism of SH on A375 cells, flow cytometry was conducted to assess whether the anti-proliferative effect of SH on A375 cells was mediated by cell cycle arrest. Under the higher inhibitory concentrations of 200 and 400 µg/ml, SH significantly increased the number of cells in S phase (Fig. 2). At 200 µg/ml, SH significantly decreased the number of cells at the G_2/M phase, while the number of cells at the G_0/G_1 phase significantly decreased with 400 µg/ml SH (Fig. 2). Hence, SH mainly induced cell cycle arrest of A375 cells at the S phase.

Flow cytometry with Annexin V-FITC and PI staining was then used to examine the contribution of apoptosis to the SH-mediated inhibition of cell proliferation. SH treatment significantly increased early apoptotic, late apoptotic and necrotic cells compared with the control group (Fig. 3). Hence, S-phase arrest and apoptosis may be mainly involved in the anti-proliferative effect of SH on A375 cells.

SH induces S phase arrest via p21-cyclin-CDK complex signalling pathways. To further elaborate the molecular mechanism underpinning the anti-proliferative action of SH, RT-qPCR analysis was performed using A375 cells treated with 400 µg/ml SH for 6 and 48 h, since 400 µg/ml SH exhibited an increased ability of S phase arrest. A number of key genes involved in cell cycle were analysed. As shown in Fig. 4A,

the expression levels of *p21* were significantly upregulated, whereas those of *p27*, *CyclinsA*, *C*, *D* and *E*, and *CDK1*, *2*, *4*, *5* and *6* were significantly downregulated after 48 h of SH treatment. No significant difference was observed in the expression levels of *TGFB*, *Smad2*, *Smad4*, *p53*, *CyclinB*, *CDK3*, *CDK7* and *Rb*. Additionally, transcription factors *E2F1* and *DP1* were significantly downregulated after 48 h of SH treatment.

To confirm the difference in gene expression, western blot and immunofluorescence analyses were conducted. As shown in Fig. 4B, the expression levels of the proteins encoded by some of the aforementioned key genes, such as p21, CyclinD, CDK2, CDK4 and CDK6, were consistent with their gene expression levels after 48 h of SH treatment. Immunofluorescence analysis of CyclinD-stained cells revealed that the green fluorescence signals in nuclei were strong without SH treatment, while after treatment with 400 µg/ml SH for 48 h, the number of cells decreased markedly compared with the control, and the green fluorescence signals were weaker (Fig. 4C). Therefore, SH may inhibit A375 cell proliferation by inducing cell cycle arrest at the S phase by upregulating p21 expression, which inhibits the expression levels of cyclin-CDK complexes.

SH induces apoptosis by downregulating Bcl-2 expression. Several key genes involved in apoptosis were analysed by RT-qPCR analysis using A375 cells treated with 400 µg/ml SH for 6 and 48 h, since 400 µg/ml SH strongly induced apoptosis. The relative mRNA expression levels of pro-apoptotic genes (*Bad*, *Bik*, *Bid*, *Bim* and *Bak*) decreased under SH treatment. The expression levels of *Bik* and *Bim* decreased at 6 h significantly, *Bid* and *Bak* were downregulated at 48 h significantly, and the relative mRNA expression levels of *Bad* decreased at 6 and 48 h significantly (Fig. 5A). No significant difference was observed in the expression levels of MAPK signalling pathway-associated genes (*Ras*, *Raf*, *MEK1* and *ERK1*; Fig. 5A). The anti-apoptotic gene *Bcl-2* was significantly downregulated
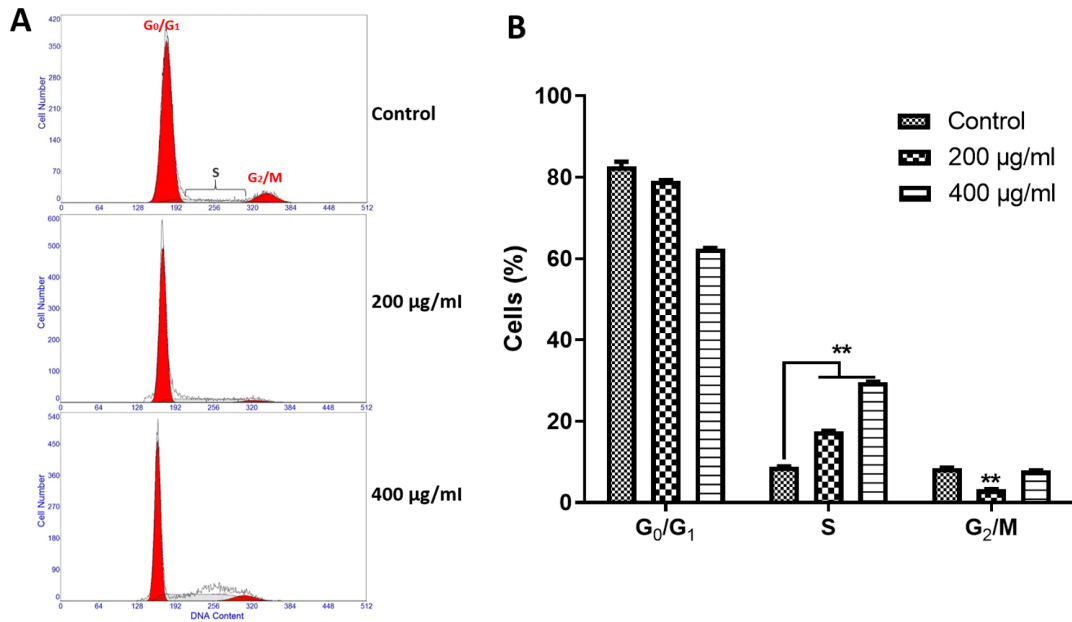
Figure 2. Cell cycle analysis of A375 cells. (A) Cell-cycle distribution was based on 2N and 4N DNA content for DNA content analysis using MultiCycle AV software. (B) Percentage of cells at different cell cycle phases. **P<0.01 vs. control. The analyses were performed in three duplicates for statistical evaluation. SH, *Sanghuangporus vaninii* extract.
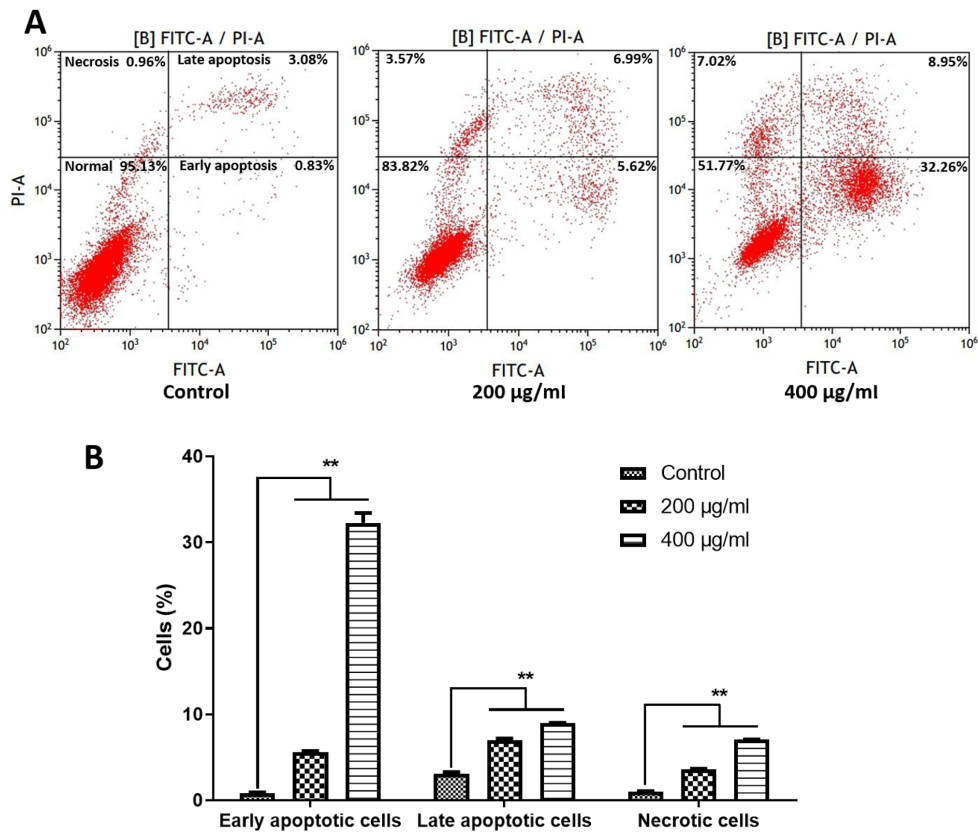

Figure 3. Apoptosis analysis of A375 cells. (A) Different groups of cells were stained with FITC-conjugated Annexin V and PI, and apoptosis was determined by flow cytometry. (B) Percentage of different types of cells. **P<0.01 vs. control. The analyses were performed in three duplicates for statistical evaluation. SH, *Sanghuangporus vaninii* extract.

after SH treatment at 48 h (Fig. 5A), consistent with the western blot analysis indicating significantly decreased Bcl-2 protein expression (Fig. 5B). Immunofluorescence analysis of Bcl-2-stained cells indicated that the cell density decreased markedly after treatment with 400 μg/ml SH for 48 h, and the green fluorescence signals were weaker than in the control group (Fig. 5C). The current results suggested that SH may induce apoptosis by downregulating Bcl-2 expression.
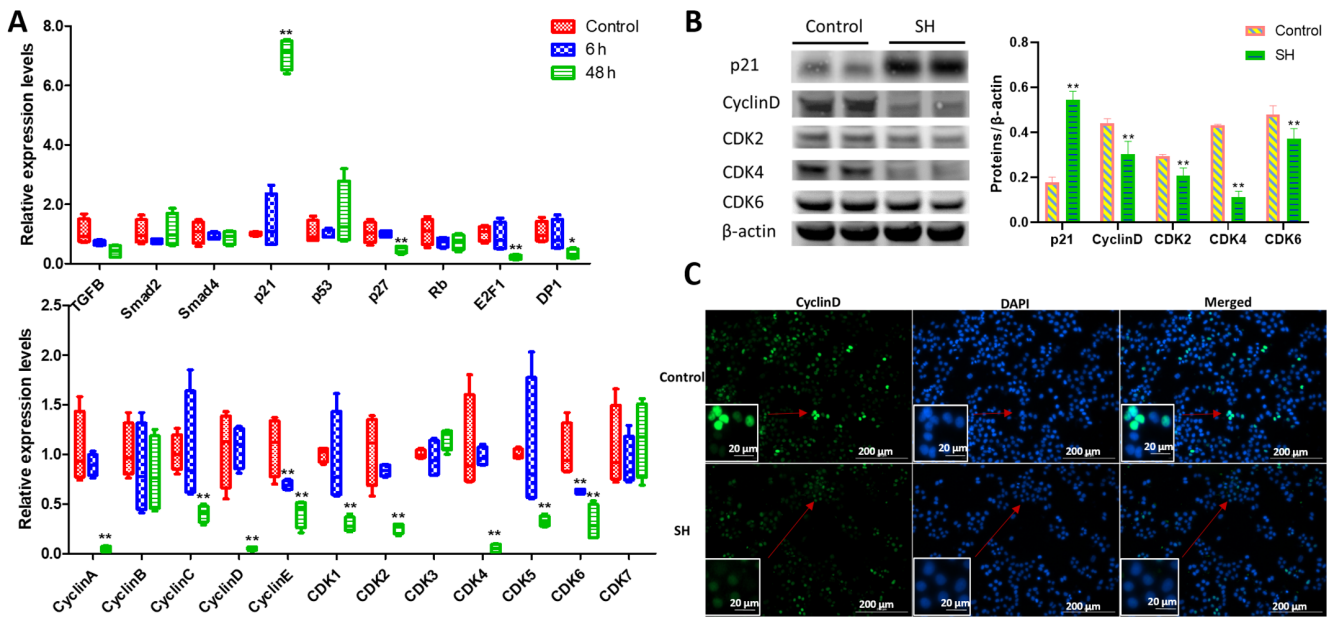
Figure 4. Analysis of cell cycle arrest-associated genes in A375 cells. (A) Reverse transcription-quantitative PCR analysis of cell cycle arrest-associated genes in A375 cells following treatment with SH (400 µg/ml) for 6 and 48 h. (B) Western blot analysis of cell cycle arrest-associated proteins in A375 cells following treatment with SH (400 µg/ml) for 48 h. (C) Immunofluorescence analysis of CyclinD in A375 cells following treatment with SH (400 µg/ml) for 48 h. Data are presented as the mean ± SD from four biological duplicates per group. *P<0.05 and **P<0.01 vs. the control. SH, aqueous extracts of *Sanghuangporus vaninii*; CDK, cyclin-dependent kinase; E2F1, transcription factor E2F1; DP1, transcription factor DP-1.
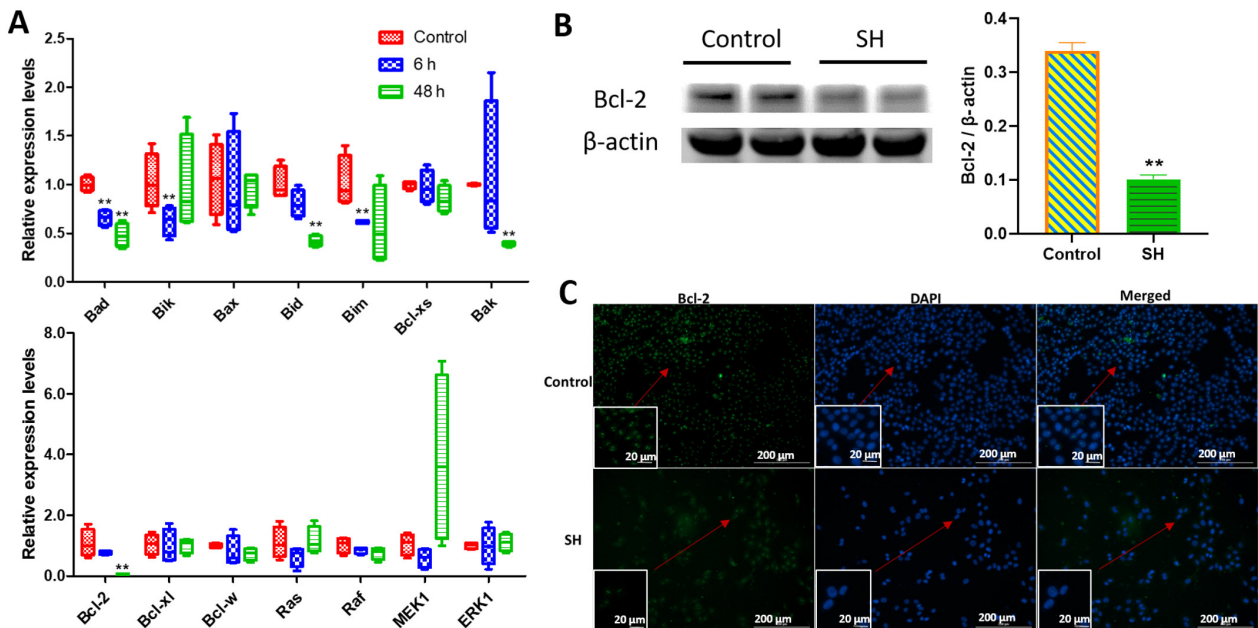

Figure 5. Analysis of apoptosis-associated genes in A375 cells. (A) Reverse transcription-quantitative PCR analysis of apoptosis-associated genes in A375 cells following treatment with SH (400 µg/ml) for 6 and 48 h. (B) Western blot analysis of Bcl-2 expression in A375 cells following treatment with SH (400 µg/ml) for 48 h. (C) Immunofluorescence analysis of Bcl-2 in A375 cells following treatment with SH (400 µg/ml) for 48 h. Data are presented as the mean ± SD from four biological duplicates per group. **P<0.01 vs. the control. SH, aqueous extracts of *Sanghuangporus vaninii*.

Discussion

Melanoma is one of the most aggressive types of cancer. No specific treatment has been developed to cure patients with metastasis (1). Natural products are important sources for the identification of novel drugs for the treatment of various diseases due to their low toxicity and compelling efficacy (19). Sanghuang mushrooms grow mainly on wild mulberry tree trunks and possess multifunctional bioactivities, such as anti-carcinogenesis, anti-fungal and immunomodulatory activities, as well as anti-diabetic/hyperlipidaemic effects (5,6), presenting Sanghuang as a potential natural product reservoir. Extracts from *S. gilvus* and *S. baumii* inhibit murine or human melanoma cell proliferation both *in vitro* and *in vivo* (10,15,16). However, to the best of our knowledge, whether *S. vaninii* affects melanoma development has not been revealed. In the present
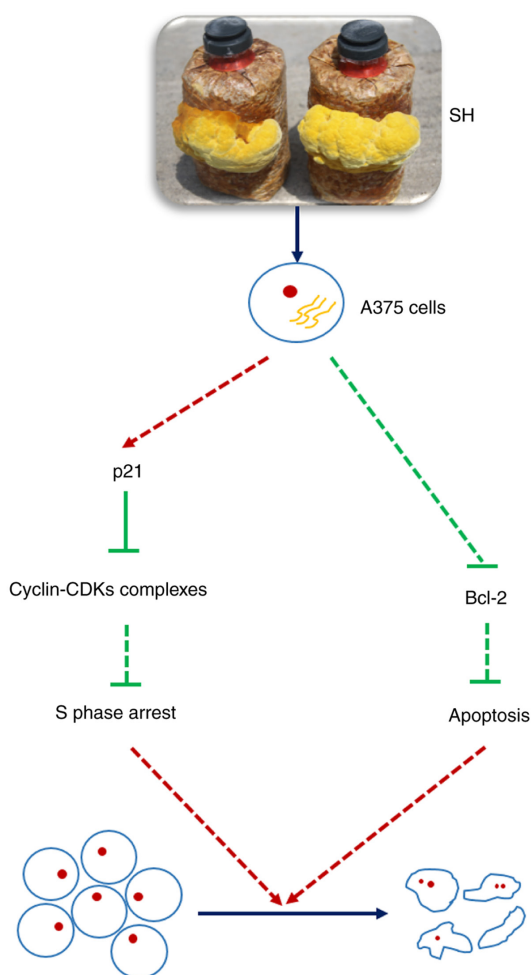
Figure 6. Proposed regulatory mechanism of SH on A375 cells. SH, aqueous extracts of *Sanghuangporus vaninii*; CDK, cyclin-dependent kinase.

study, it was revealed that aqueous extracts of *S. vaninii* (SH) exerted a proliferation inhibitory effect on human melanoma cells, providing an alternative Sanghuang candidate for developing effective interventions against melanoma.

In general, cancer is well-characterised by continuous cell proliferative ability; hence, interruptions on cancer cell cycle may hinder cancer development (20). In the present study, the effects of SH on melanoma A375 cell proliferation were assessed by MTT assay, revealing that SH exerted a prominent anti-proliferative action in a dose-dependent manner. Perturbations of cell proliferation can be largely attributed to abnormal modulations on cell cycle and apoptosis. Therefore, flow cytometry assays were performed to determine the underlying mechanism. Notably, SH treatment induced cell cycle arrest at the S phase, as exhibited by the increased cell number at the S phase and decreased cell number at the G_0/G_1 phase, suggesting that SH may act as a potential proliferation inhibitor of melanoma cells. Consistently with the current results, *S. baumii* can suppress the proliferation of human melanoma A375 cells by promoting cell cycle arrest at the S phase (15). Moreover, protocatechualdehyde isolated from *S. gilvus* can induce cell cycle arrest in HT29 and B16F10 cells (12,16). Overall, cell cycle arrest may be the general regulatory mechanism of Sanghuang family members in inhibiting the proliferation of cancer cells.

The cell cycle is highly orchestrated by a series of events and signalling pathways, among which cyclins and CDKs are essential in mediating the cell cycle (21). The activity of CDKs is mainly regulated by binding of cyclin proteins/CDK inhibitors and phosphorylation. High levels of p21, also known as CDK inhibitor 1A, can inhibit the functions of CyclinD-CDK4/6, CyclinE-CDK2 and CyclinA-CDK2 complexes, leading to the interruption of the cell cycle (20,22). Moreover, p21 participates in multiple tumour suppressor pathways, including p53-dependent and -independent mechanisms (20,22). p53 is a transcription factor that functions as a well-known tumour suppressor and is involved in both the G_0/G_1 and G_2/M cell cycle phases (23). In our previous study, it has been demonstrated that protocatechualdehyde isolated from *S. givlvus* induces S-phase arrest in HT-29 cells via the activation of the CyclinD1/E-CDK2 signalling pathway (12). To investigate the regulatory mechanism of SH on cell cycle arrest in A375 cells, the expression levels of cell cycle arrest-associated genes were assessed via RT-qPCR, western blot and immunofluorescence analyses. *p21* was significantly upregulated, and *CyclinD-CDK4/6*, *CyclinE-CDK2* and *CyclinA-CDK2* complexes were downregulated in A375 cells. No significant differences were observed in the relative mRNA expression levels of *p53* and upstream genes (*TGFB*, *Smad2* and *Smad4*) under SH treatment, suggesting that SH may promote p21 expression independently of p53 signalling. The expression levels of *E2F1* and *DP1* were significantly decreased after 48 h of treatment, and this may be caused by the downregulation of *CyclinA* and *CDK1*. Therefore, the current results suggested that SH treatment in A375 cells upregulated *p21* expression to inhibit Cyclin-CDK complexes, resulting in cell cycle arrest at the S phase.

Apoptosis is an evolutionarily conserved process that serves an essential role in organism development and tissue homeostasis (24). However, cancer cells lose their ability to undergo apoptosis-induced death, leading to uncontrolled proliferation. It has been previously demonstrated that protocatechualdehyde isolated from *S. gilvus* induces apoptosis in HT-29 and B16F10 cells (12,16). In the present study, SH induced apoptosis in A375 cells. Under SH treatment, the expression levels of pro-apoptotic genes, such as *Bad*, *Bik*, *Bid*, *Bim* and *Bak*, decreased to varying extents, and the anti-apoptotic gene *Bcl-2* was significantly inhibited. The Bcl-2 protein family is the key regulator of the intrinsic apoptosis pathway (25). Apoptosis is triggered by pro-apoptotic genes, such as *Bim* and *Bid*. This pro-apoptotic chain of events is countered by the anti-apoptotic genes *Bcl-2*, *Bcl-xl* and *Bcl-w*, which can block apoptosis by binding and sequestering pro-apoptotic proteins (25). Therefore, the significant decrease of Bcl-2 may lead to apoptosis, even though the expression levels of some pro-apoptotic genes were slightly downregulated. These controversial but interesting results require further research.

The current findings suggested that SH induced S-phase arrest via p21-cyclin-CDKs complex pathways, and induced apoptosis by inhibiting the expression levels of Bcl-2 (Fig. 6). Specific information about the active component(s) in aqueous extracts of *S. vaninii* should be obtained in future studies on isolation, identification and illustration. In addition, the anti-proliferative effects of SH on human melanoma cells *in vivo* should be further investigated in future studies.

In conclusion, the present study revealed that the aqueous extracts of *S. vaninii* fruiting body effectively inhibited the proliferation of human melanoma cells by inducing cell cycle arrest at the S phase, and this arrest may be mediated by the activation of the p21-Cyclin-CDKs complexes signaling pathways. Additionally, SH induced apoptosis of A375 cells via significantly inhibiting the expression levels of the anti-apoptotic gene *Bcl-2* (Fig. 6). The current results suggested that *S. vaninii* fruiting body may be used as a source of drug development for the prevention and treatment of melanoma.

Acknowledgements

Not applicable.

Availability of data and materials

The datasets used and/or analyzed during the current study are available from the corresponding author on reasonable request.

Authors' contributions

TY, LL and JH contributed to the conception of the study. SZ, YS, HS, WC, JZ and YL performed the experiments. JH and LL revised the paper and gave final approval. TY, LL and JH are responsible for confirming the authenticity of the data. All authors read and approved the final manuscript.

Ethics approval and consent to participate

Not applicable.

Patient consent for publication

Not applicable.

Competing interests

The authors declare that they have no competing interests.

References

1. Olbryt M: Molecular background of skin melanoma development and progression: Therapeutic implications. Postepy Dermatol Alergol 36: 129-138, 2019.
2. Davis LE, Shalin SC and Tackett AJ: Current state of melanoma diagnosis and treatment. Cancer Biol Ther 20: 1366-1379, 2019.
3. Lee JH, Cho SM, Kim HM, Hong ND and Yoo ID: Immunostimulating activity of polysaccharides from mycelia of Phellinus linteus grown under different culture conditions. J Microbiol Biotechnol 7: 2-55, 1997.
4. Chen H, Tian T, Miao H and Zhao YY: Traditional uses, fermentation, phytochemistry and pharmacology of Phellinus linteus: A review. Fitoterapia 113: 6-26, 2016.
5. Chen W, Tan H, Liu Q, Zheng X, Zhang H, Liu Y and Xu L: A review: The bioactivities and pharmacological applications of Phellinus linteus. Molecules 24: 1888, 2019.
6. Huo J, Zhong S, Du X, Cao Y, Wang W, Sun Y, Tian Y, Zhu J, Chen J, Xuan L, et al: Whole-genome sequence of Phellinus gilvus (mulberry Sanghuang) reveals its unique medicinal values. J Adv Res 24: 325-335, 2020.
7. Meera CR, Janardhanan KK and Karunagaran D: Antiproliferative and apoptotic activities of the medicinal mushroom Phellinus rimosus (Agaricomycetes) on HCT116 human colorectal carcinoma cells. Int J Med Mushrooms 20: 935-945, 2018.
8. Wang FF, Shi C, Yang Y, Fang Y, Sheng L and Li N: Medicinal mushroom Phellinus igniarius induced cell apoptosis in gastric cancer SGC-7901 through a mitochondria-dependent pathway. Biomed Pharmacother 102: 18-25, 2018.
9. Im KH, Baek SA, Choi J and Lee TS: Antioxidant, anti-melanogenic and anti-wrinkle effects of Phellinus vaninii. Mycobiology 47: 494-505, 2019.
10. Bae JS, Jang KH, Yim H and Jin HK: Polysaccharides isolated from Phellinus gilvus inhibit melanoma growth in mice. Cancer Lett 218: 43-52, 2005.
11. Bae JS, Jang KH, Yim H, Park SC and Jin HK: Inhibitory effects of polysaccharides isolated from Phellinus gilvus on benzo(a)pyrene-induced forestomach carcinogenesis in mice. World J Gastroenterol 11: 577-579, 2005.
12. Zhong S, Li YG, Ji DF, Lin TB and Lv ZQ: Protocatechualdehyde induces S-phase arrest and apoptosis by stimulating the p27KIP1-Cyclin A/D1-CDK2 and mitochondrial apoptotic pathways in HT-29 Cells. Molecules 21: 934, 2016.
13. Chao W, Deng JS, Li PY, Liang YC and Huang GJ: 3,4-Dihydroxybenzalactone suppresses human non-small cell lung carcinoma cells metastasis via suppression of epithelial to mesenchymal transition, ROS-mediated PI3K/AKT/MAPK/MMP and NFκB signaling pathways. Molecules 22: 537, 2017.
14. Liu YJ, Lyu JL, Kuo YH, Chiu CY, Wen KC and Chiang HM: The anti-melanogenesis effect of 3,4-dihydroxybenzalacetone through downregulation of melanosome maturation and transportation in B16F10 and human epidermal melanocytes. Int J Mol Sci 22: 2823, 2021.
15. Yang Y, Zhang L, Chen Q, Lu WL and Li N: Antitumor effects of extract of the oak bracket medicinal mushroom, Phellinus baumii (Agaricomycetes), on human melanoma cells A375 in vitro and in vivo. Int J Med Mushrooms 22: 197-209, 2020.
16. Zhong S, Jin Q, Yu T, Zhu J and Li Y: Phellinus gilvus derived protocatechualdehyde induces G0/G1 phase arrest and apoptosis in murine B16 F10 cells. Mol Med Rep 21: 1107-1114, 2020.
17. Huo J, Sun Y, Zhong S, Li Y, Yang R, Xia L, Wang J, Zhang M and Zhu J: Safety evaluation of aqueous extracts of Sanghuangporus vaninii fruiting body in Sprague-Dawley rats. Food Sci Nutr 8: 5107-5113, 2020.
18. Schmittgen TD and Livak KJ: Analyzing real-time PCR data by the comparative C(T) method. Nat Protoc 3: 1101-1108, 2008.
19. Harvey AL, Edrada-Ebel R and Quinn RJ: The re-emergence of natural products for drug discovery in the genomics era. Nat Rev Drug Discov 14: 111-129, 2015.
20. Moussa RS, Park KC, Kovacevic Z and Richardson DR: Ironing out the role of the cyclin-dependent kinase inhibitor, p21 in cancer: Novel iron chelating agents to target p21 expression and activity. Free Radic Biol Med 133: 276-294, 2019.
21. Diaz-Moralli S, Tarrado-Castellarnau M, Miranda A and Cascante M: Targeting cell cycle regulation in cancer therapy. Pharmacol Ther 138: 255-271, 2013.
22. Al Bitar S and Gali-Muhtasib H: The role of the cyclin dependent kinase inhibitor p21cip1/waf1 in targeting cancer: Molecular mechanisms and novel therapeutics. Cancers (Basel) 11: E1475, 2019.
23. Golias CH, Charalabopoulos A and Charalabopoulos K: Cell proliferation and cell cycle control: A mini review. Int J Clin Pract 58: 1134-1141, 2004.
24. Du Toit A: Cell death: Balance through a bivalent regulator. Nat Rev Mol Cell Biol 14: 546-547, 2013.
25. Singh R, Letai A and Sarosiek K: Regulation of apoptosis in health and disease: The balancing act of BCL-2 family proteins. Nat Rev Mol Cell Biol 20: 175-193, 2019.